Supplementary Material

Effect of Bisphenol A on Craniofacial Cartilage Development in Zebrafish (*Danio rerio*) Embryos: A Morphological Study

Wenlong Huang [a], Xin Wang [a], Shukai Zheng [a], Ruotong Wu [b], Caixia Liu [a], Kusheng Wu [a, c, *]

[a] Department of Preventive Medicine, Shantou University Medical College, Shantou 515041, Guangdong, China

[b] School of Life Science, Xiamen University, Xiamen 361102, Fujian, China

[c] Guangdong Provincial Key Laboratory of Breast Cancer Diagnosis and Treatment, Shantou 515041, Guangdong, China

*Corresponding author:

Kusheng Wu, Ph.D.

Department of Preventive Medicine, Shantou University Medical College

Guangdong Provincial Key Laboratory of Breast Cancer Diagnosis and Treatment

No.22, Xinling Rd. Shantou 515041, Guangdong, China

E-mail address: kswu@stu.edu.cn

	Figure annotation	Receptor/ enzyme
Fig. S1	Pharyngeal cartilage of zebrafish.	
Fig. S2	Graphic representation of mRNA abundance changes of genes associated to craniofacial development/skeletal formation, steroid hormone biosynthesis and metabolism of xenobiotics by cytochrome p450.	
Fig. S3	Ocular and craniofacial malformations in zebrafish larvae after BPA exposure.	
Fig. S4	Angle and length measured in 5-dpf zebrafish co-exposed from 0-5 dpf to 0.05 μM BPA+ 1.0 μM ICI (**broad ER antagonist**).	**ER**
Fig. S5	Angle and length measured in 5-dpf zebrafish co-exposed from 0-5 dpf to 0.1 μM BPA+ 1.0 μM ICI (**broad ER antagonist**).	
Fig. S6	Angle and length measured in 5-dpf zebrafish co-exposed from 0-5 dpf to 0.05 μM BPA+ 1.0 μM AZD (**ERα antagonist**).	**ERα**
Fig. S7	Angle and length measured in 5-dpf zebrafish co-exposed from 0-5 dpf to 0.1 μM BPA+ 1.0 μM AZD (**ERα antagonist**).	
Fig. S8	Angle and length measured in 5-dpf zebrafish co-exposed from 0-5 dpf to 0.05 μM BPA+ 1.0 μM PHTPP (**ERβ antagonist**).	**ERβ**
Fig. S9	Angle and length measured in 5-dpf zebrafish co-exposed from 0-5 dpf to 0.1 μM BPA+ 1.0 μM PHTPP (**ERβ antagonist**).	
Fig. S10	Angle and length measured in 5-dpf zebrafish co-exposed from 0-5 dpf to 0.05 μM BPA+ 1.0 μM FAD (**Aromatase B inhibitor**).	**Aromatase B**
Fig. S11	Angle and length measured in 5-dpf zebrafish co-exposed from 0-5 dpf to 0.1 μM BPA+ 1.0 μM FAD (**Aromatase B inhibitor**).	
Fig. S12	Angle and length measured in 5-dpf zebrafish exposed from 0-5 dpf to 0.05 μM BPA or 0.1 μM GSK4716 (**ERR agonist**) alone.	**ERR**
Fig. S13	Angle and length measured in 5-dpf zebrafish exposed from 0-5 dpf to 0.1 μM BPA or 0.1 μM GSK4716 (**ERR agonist**) alone.	
Fig. S14	Angle and length measured in 5-dpf zebrafish co-exposed from 0-5 dpf to 0.05 μM BPA+ 6.17 μM FLU (**AR inhibitor**).	**AR**
Fig. S15	Angle and length measured in 5-dpf zebrafish co-exposed from 0-5 dpf to 0.1 μM BPA+ 6.17 μM FLU (**AR inhibitor**).	
Fig. S16	Angle and length measured in 5-dpf zebrafish co-exposed from 0-5 dpf to 0.05 μM BPA+ 1.0 μM AMO (**THR antagonist**).	**THR**
Fig. S17	Angle and length measured in 5-dpf zebrafish co-exposed from 0-5 dpf to 0.1 μM BPA+ 1.0 μM AMO (**THR antagonist**).	

Method

Global transcriptome sequencing dataset (GSE113676) was downloaded from Gene Expression Omnibus (GEO) database. We mainly focused on gene expression profile involved in craniofacial development/skeletal formation, steroid hormone biosynthesis and metabolism of xenobiotics by cytochrome p450.

Table S1. Receptor/enzyme inhibitors used for co-exposure experiment

Receptor/enzyme inhibitor or agonist	Receptor/enzyme	CAS NO.	Purity	Used concentration*
Fulvestrant (ICI)	ER	129453-61-8	99.99%	1 μM
AZD9496 (AZD)	ERα	1639042-08-2	99.15%	1 μM
PHTPP	ERβ	805239-56-9	99.64%	1 μM
Fadrozole (FAD)	Aromatase B	102676-47-1	99.78%	1 μM
Flutamide (FLU)	AR	13311-84-7	99.77%	6.17 μM
Amiodarone (AMO)	ThRα/ThRβ transcriptional	19774-82-4	99.67%	50 nM
GSK4716	ERRβ/γ	101574-65-6	98.86%	0.1 μM

*The concentrations used were according to a previous work (Kinch et al., 2015)

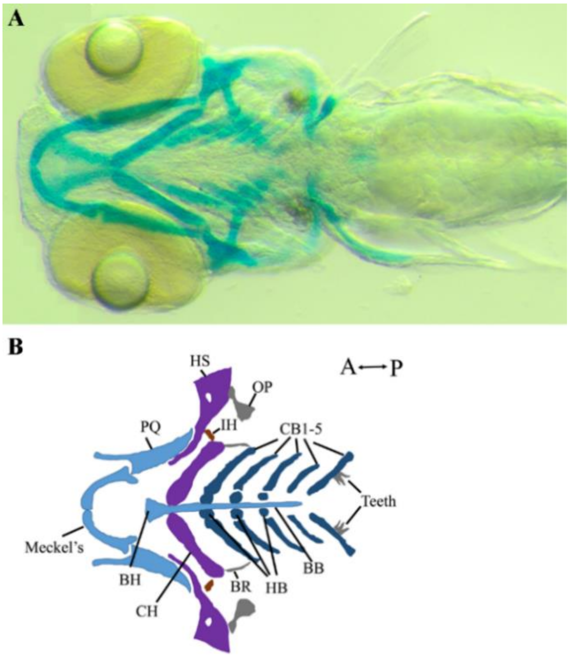

Fig. S1 Craniofacial cartilage of zebrafish. (A) Ventral view of an Alcian blue-stained larval viscerocranium, showing the skeletal derivatives of the seven pharyngeal arches. (B) Schematic of the larval viscerocranium [image was cited from (Mork and Crump, 2015), with minor modification]. First-arch structures: PQ, palatoquadrate; Meckel's, Meckel's cartilage; second-arch structures: HS, hyosymplectic; IH, interhyal; CH, ceratohyal; Bh, basihyal; OP, opercle (bone); BR, branchiostegal ray (bone); arches 3–7: CB, ceratobranchial; HB, hypobranchial; BB, basibranchial.

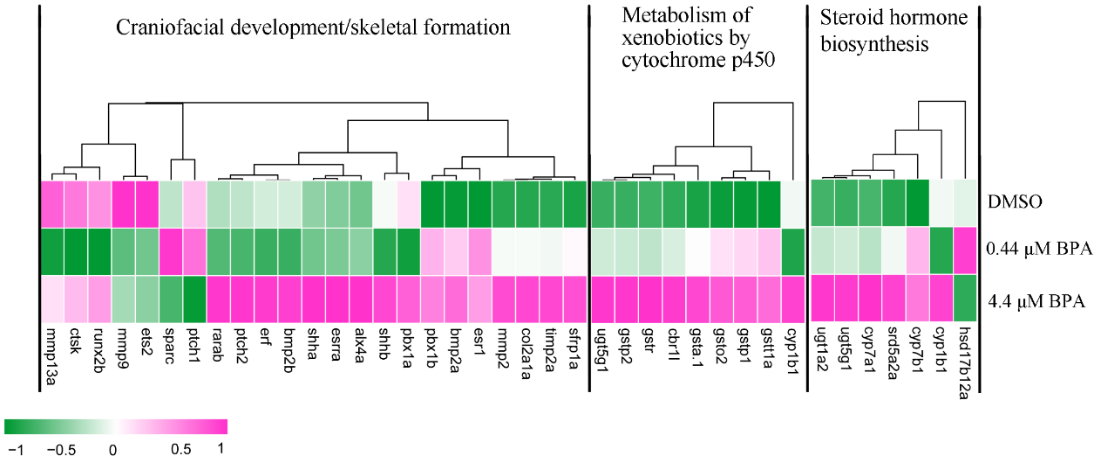

Fig. S2 Graphic representation of mRNA abundance changes of genes associated to craniofacial development/skeletal formation, steroid hormone biosynthesis and metabolism of xenobiotics by cytochrome p450. Sequencing data were downloaded from Gene Expression Omnibus (GSE113676), Red violet (up-regulated) and green dots (down-regulated) indicate genes related to corresponding pathways.

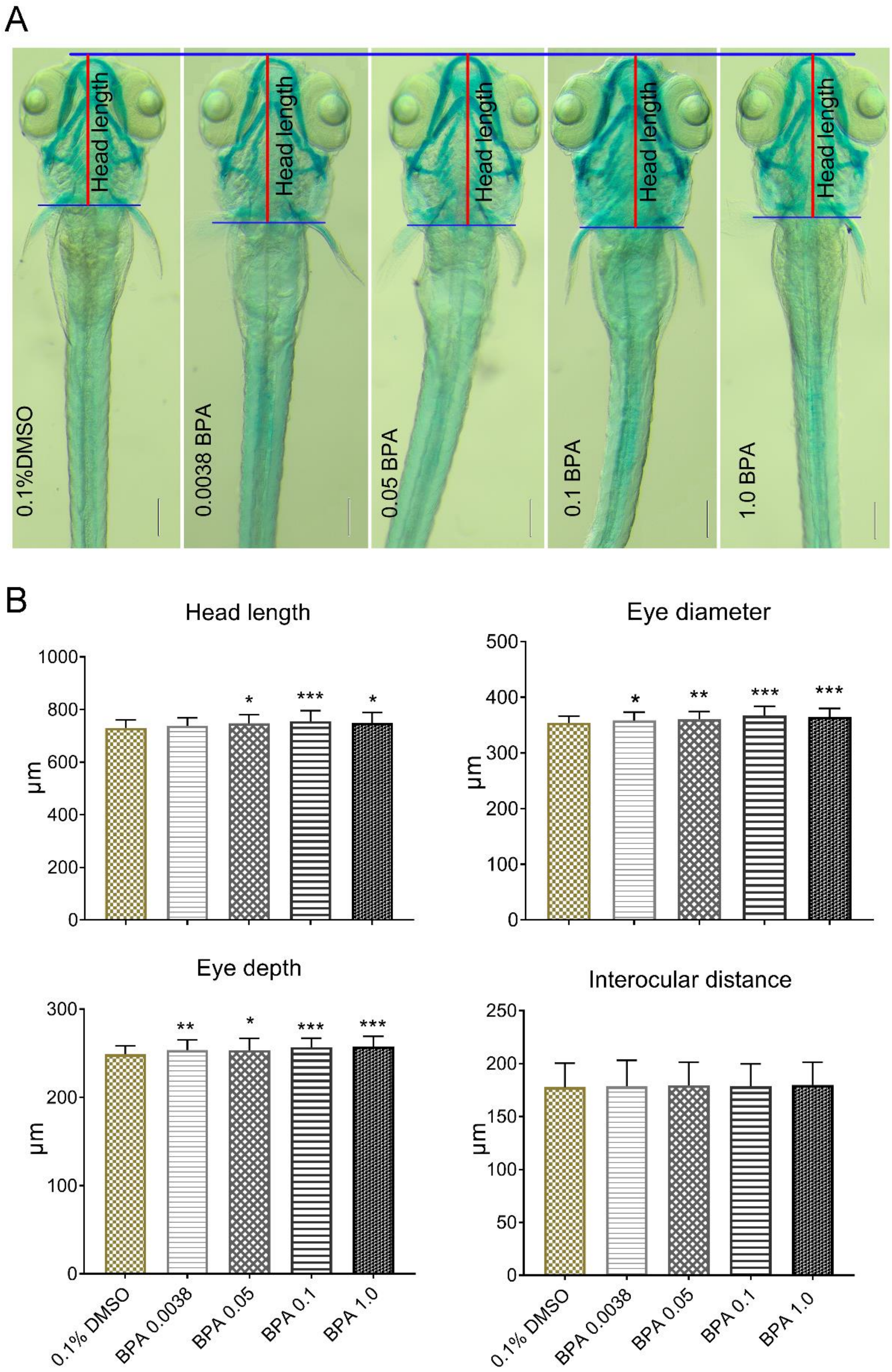

Fig. S3 Ocular and craniofacial malformations in zebrafish larvae after BPA exposure. (A) Whole-mounted preparations of the larval skull (dorsal view). (B) BPA exposure led to craniofacial abnormality. Data are presented as violin-plots (n = 12-20 for each group, 3 biological replicates), Asterisks indicate significant difference between each treatment group and control (*p < 0.05, **p < 0.01 and ***p < 0.001).

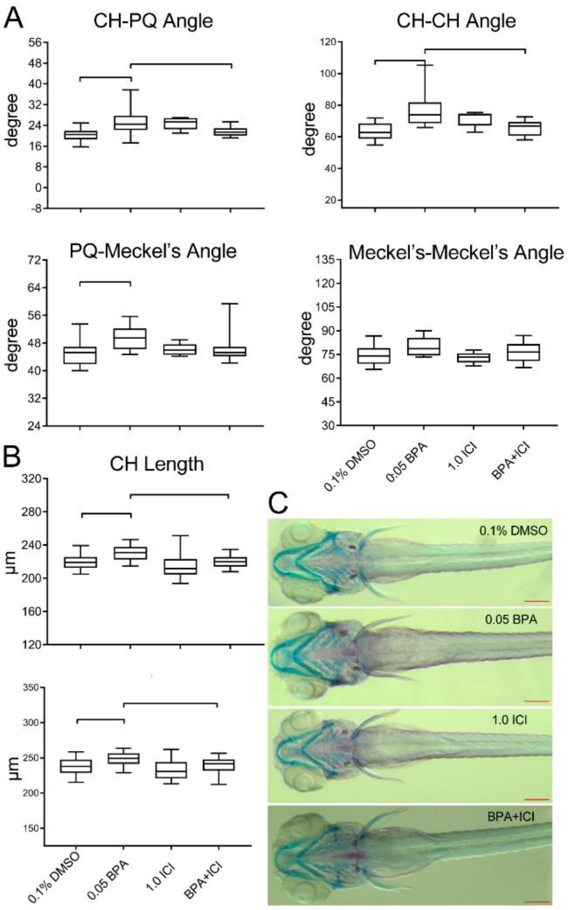

Fig. S4 Angle and length measured in 5-dpf zebrafish co-exposed from 0-5 dpf to 0.05 μM BPA+ 1.0 μM ICI. (A-C) Data are presented as box-whisker plots (n = 5-10 fish per group), tick-down line indicates significant difference. (D) Representative images of whole-mounted alcian blue stained larval skull. Scale bar: 200 μm (similarly hereinafter).

Fig. S5 Angle and length measured in 5-dpf zebrafish co-exposed from 0-5 dpf to 0.1 μM BPA+ 1.0 μM ICI. (A-C) Data are presented as box-whisker plots (n = 5-7 fish per group), tick-down line indicates significant difference. (D) Representative images of whole-mounted alcian blue stained larval skull.

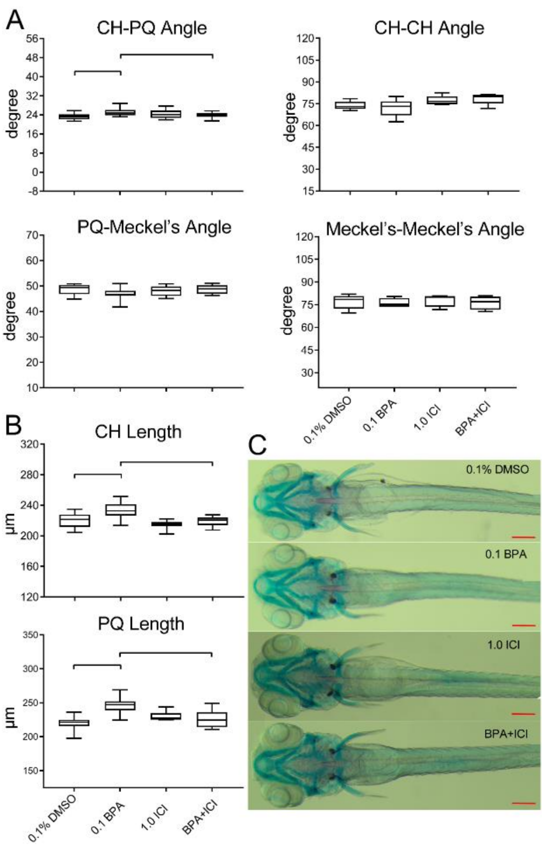

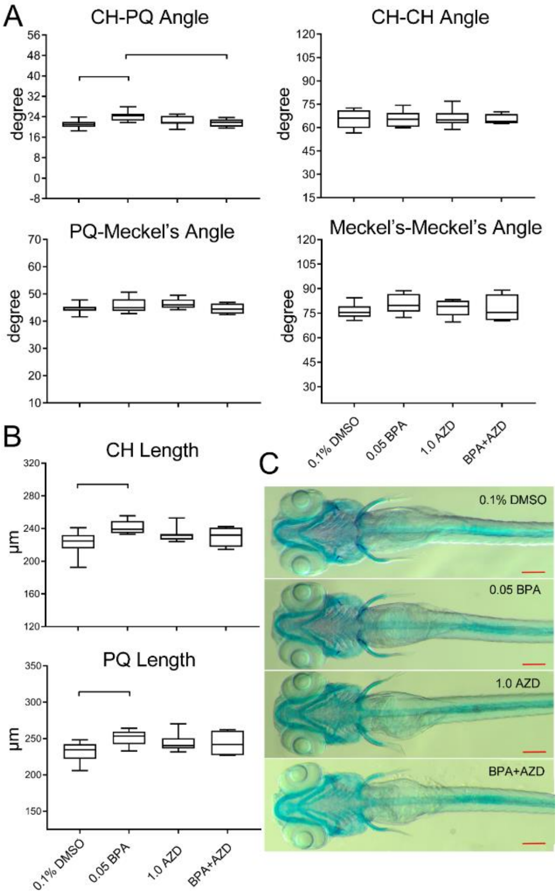

Fig. S6 Angle and length measured in 5-dpf zebrafish co-exposed from 0-5 dpf to 0.05 μM BPA+ 1.0 μM AZD. (A-C) Data are presented as box-whisker plots (n = 8-10 fish per group), tick-down line indicates significant difference. (D) Representative images of whole-mounted alcian blue stained larval skull.

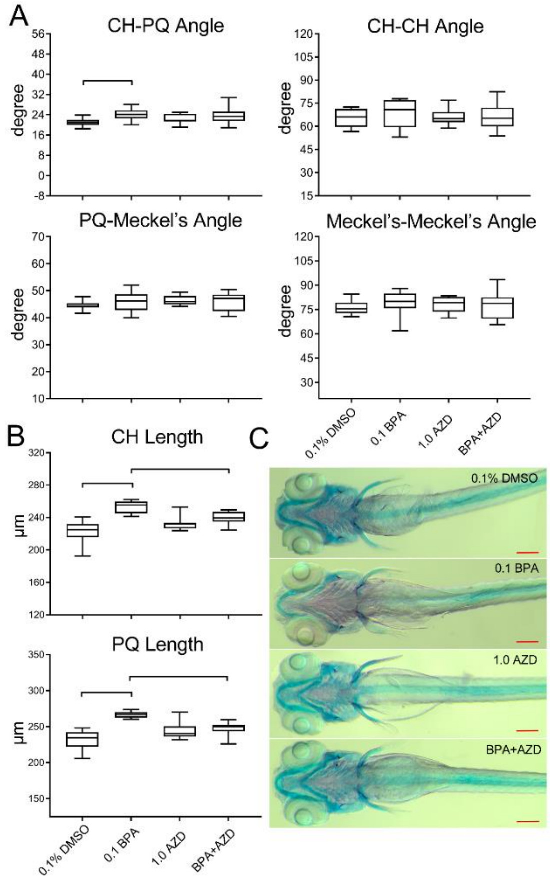

Fig. S7 Angle and length measured in 5-dpf zebrafish co-exposed from 0-5 dpf to 0.1 μM BPA+ 1.0 μM AZD. (A-C) Data are presented as box-whisker plots (n = 8-11 fish per group), tick-down line indicates significant difference. (D) Representative images of whole-mounted alcian blue stained larval skull.

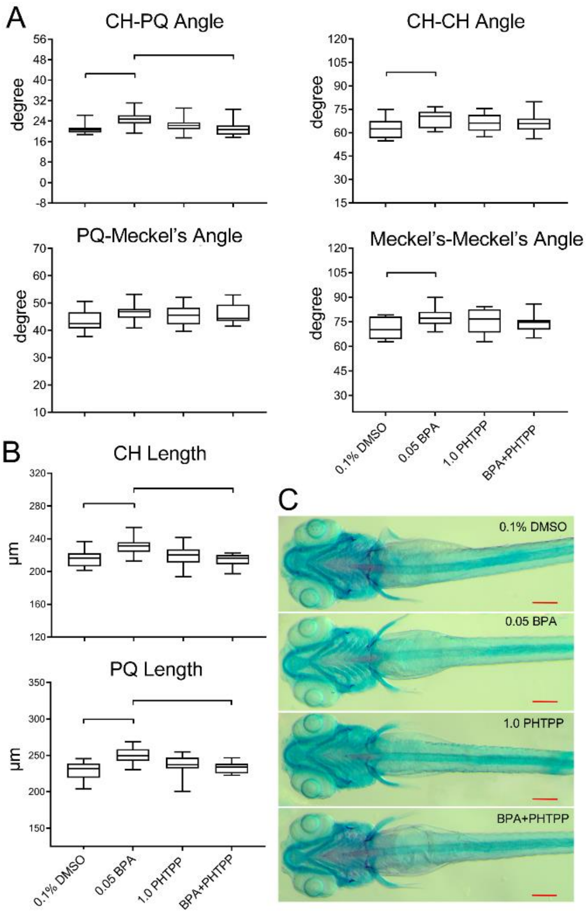

Fig. S8 Angle and length measured in 5-dpf zebrafish co-exposed from 0-5 dpf to 0.05 μM BPA+ 1.0 μM PHTPP. (A-C) Data are presented as box-whisker plots (n = 8-12 fish per group), tick-down line indicates significant difference. (D) Representative images of whole-mounted alcian blue stained larval skull.

Fig. S9 Angle and length measured in 5-dpf zebrafish co-exposed from 0-5 dpf to 0.1 μM BPA+ 1.0 μM PHTPP. (A-C) Data are presented as box-whisker plots (n = 7-12 fish per group), tick-down line indicates significant difference. (D) Representative images of whole-mounted alcian blue stained larval skull.

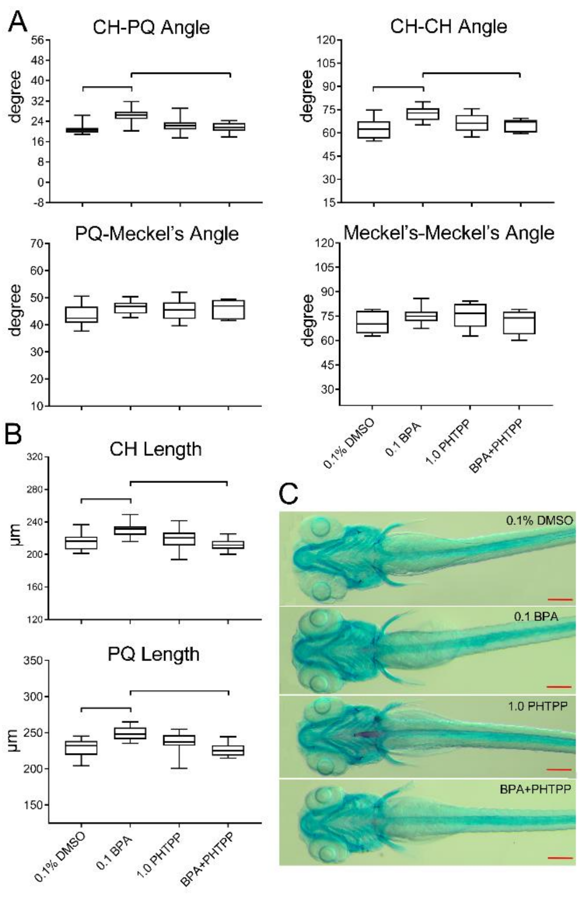

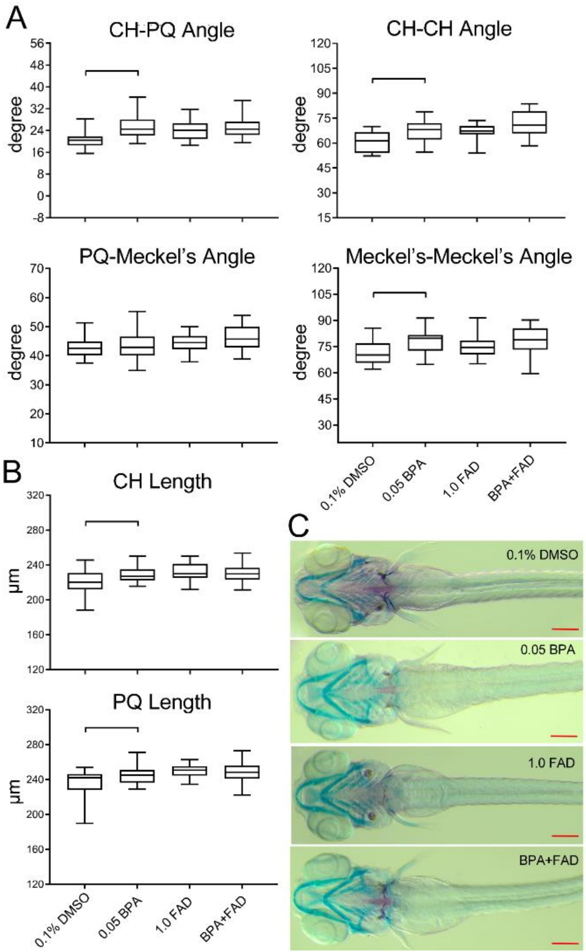

Fig. S10 Angle and length measured in 5-dpf zebrafish co-exposed from 0-5 dpf to 0.05 µM BPA+ 1.0 µM FAD. (A-C) Data are presented as box-whisker plots (n = 11-17 fish per group), tick-down line indicates significant difference. (D) Representative images of whole-mounted alcian blue stained larval skull.

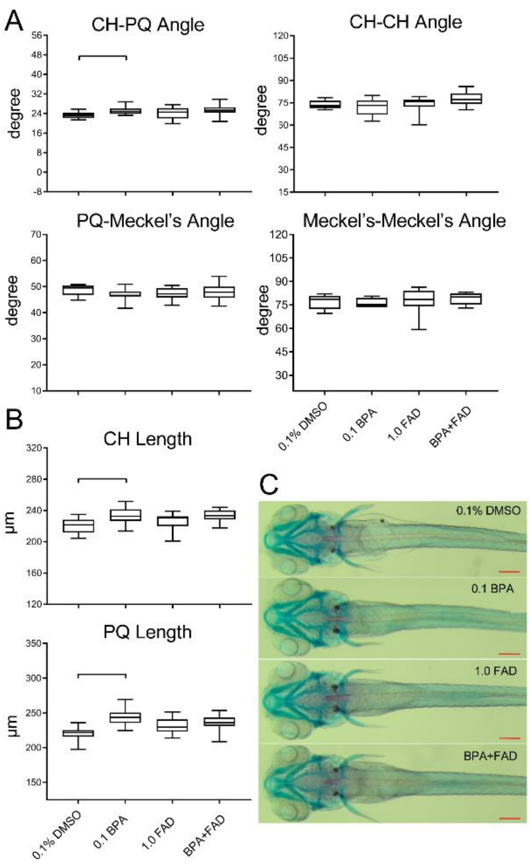

Fig. S11 Angle and length measured in 5-dpf zebrafish co-exposed from 0-5 dpf to 0.1 µM BPA+ 1.0 µM FAD. (A-C) Data are presented as box-whisker plots (n = 8-10 fish per group), tick-down line indicates significant difference. (D) Representative images of whole-mounted alcian blue stained larval skull.

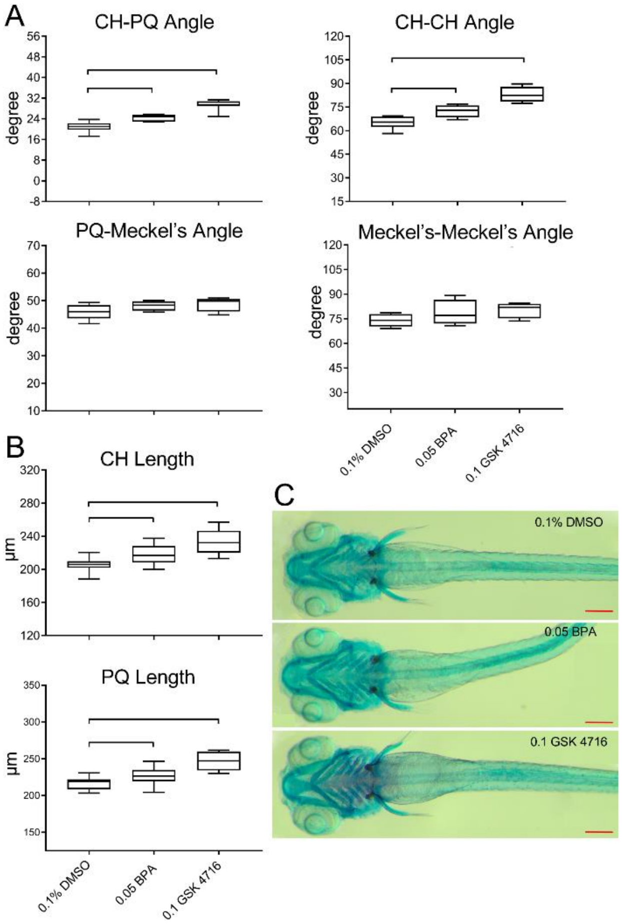

Fig. S12 Angle and length measured in 5-dpf zebrafish exposed from 0-5 dpf to 0.05 µM BPA or 0.1 µM GSK4716 alone. (A-C) Data are presented as box-whisker plots (n = 6-8 fish per group), tick-down line indicates significant difference. (D) Representative images of whole-mounted alcian blue stained larval skull.

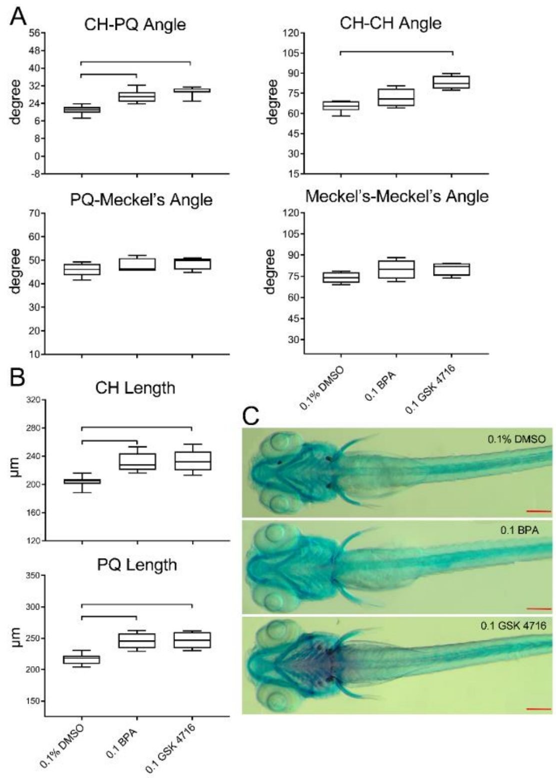

Fig. S13 Angle and length measured in 5-dpf zebrafish exposed from 0–5 dpf to 0.1 µM BPA or 0.1 µM GSK4716 alone. (A-C) Data are presented as box-whisker plots (n = 7-8 fish per group), tick-down line indicates significant difference. (D) Representative images of whole-mounted alcian blue stained larval skull.

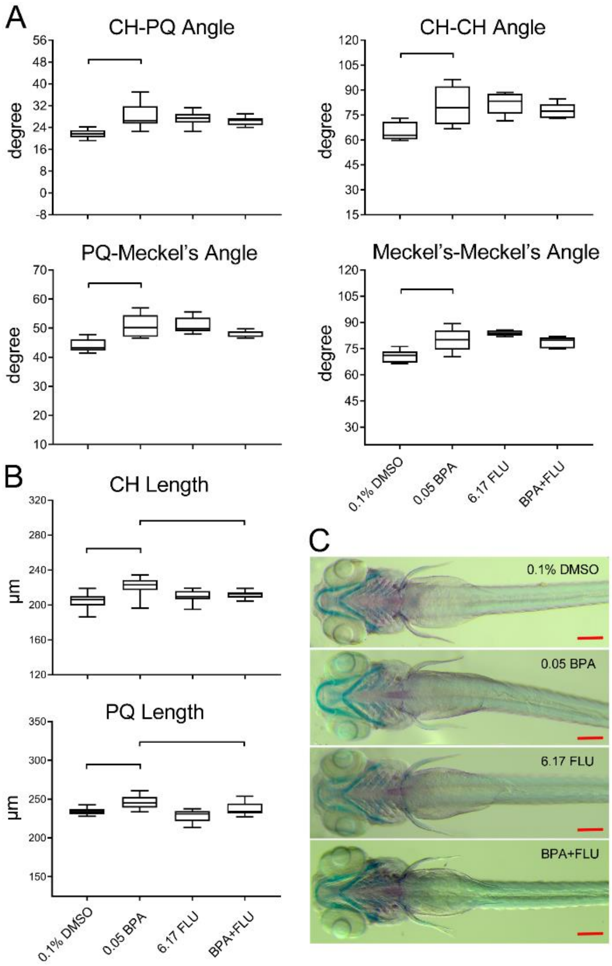

Fig. S14 Angle and length measured in 5-dpf zebrafish co-exposed from 0–5 dpf to 0.05 µM BPA+ 6.17 µM FLU. (A-C) Data are presented as box-whisker plots (n = 5-6 fish per group), tick-down line indicates significant difference. (D) Representative images of whole-mounted alcian blue stained larval skull.

Fig. S15 Angle and length measured in 5-dpf zebrafish co-exposed from 0-5 dpf to 0.1 µM BPA+ 6.17 µM FLU. (A-C) Data are presented as box-whisker plots (n = 6-10 fish per group), tick-down line indicates significant difference. (D) Representative images of whole-mounted alcian blue stained larval skull.

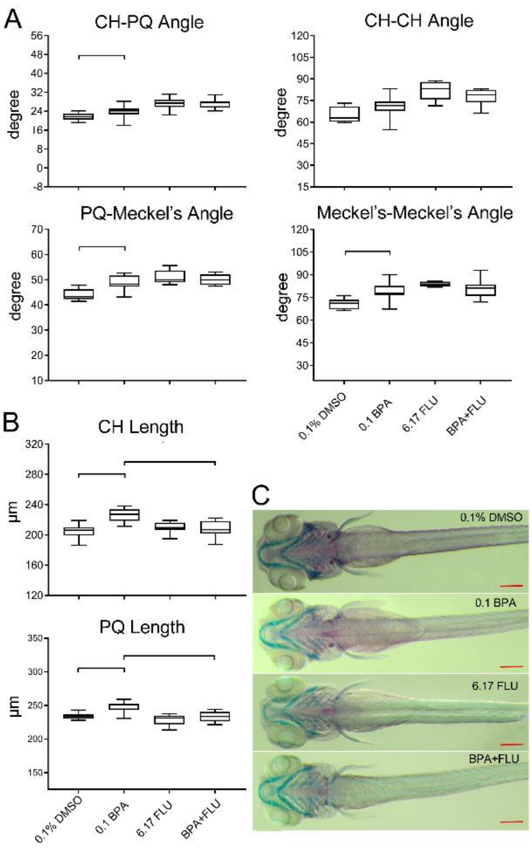

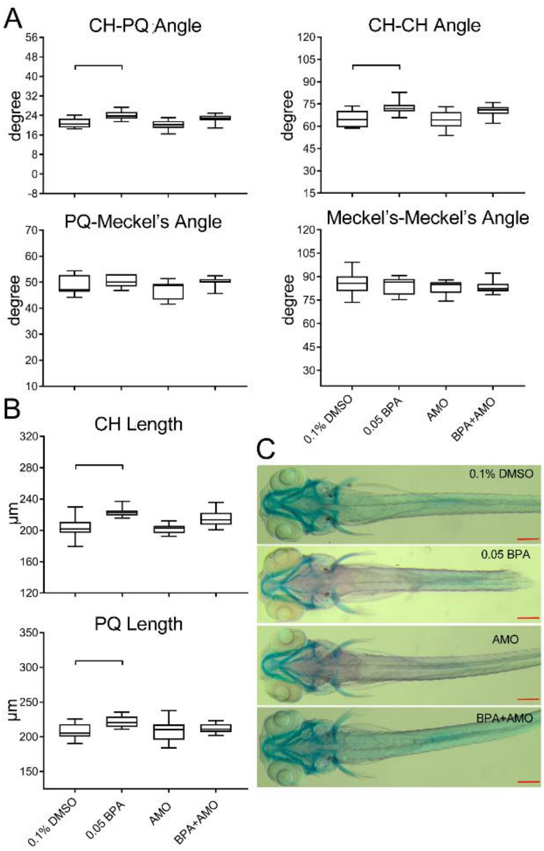

Fig. S16 Angle and length measured in 5-dpf zebrafish co-exposed from 0-5 dpf to 0.05 µM BPA+ 1.0 µM AMO. (A-C) Data are presented as box-whisker plots (n = 7-8 fish per group), tick-down line indicates significant difference. (D) Representative images of whole-mounted alcian blue stained larval skull.

Fig. S17 Angle and length measured in 5-dpf zebrafish co-exposed from 0-5 dpf to 0.1 µM BPA+ 1.0 µM AMO. (A-C) Data are presented as box-whisker plots (n = 8-10 fish per group), tick-down line indicates significant difference. (D) Representative images of whole-mounted alcian blue stained larval skull.

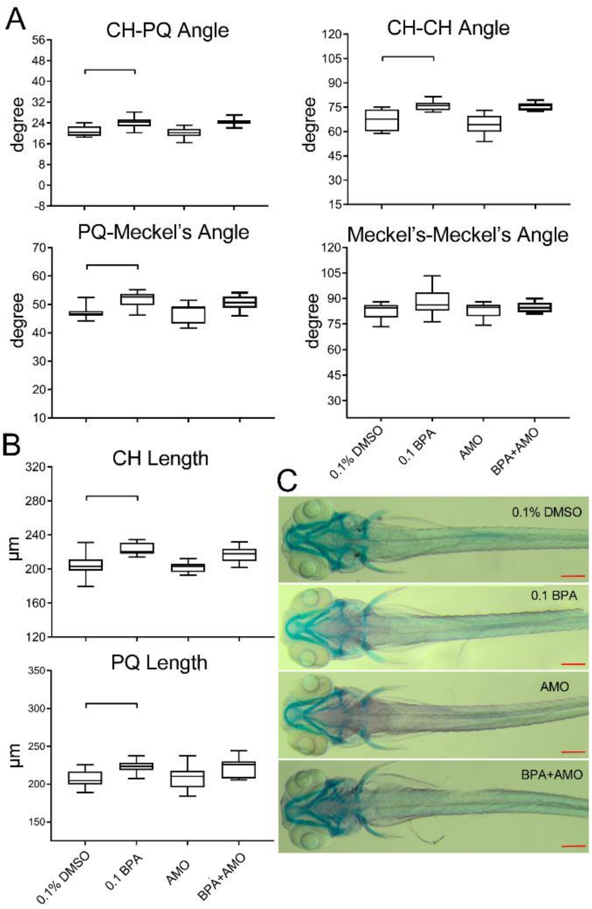

Reference:

Kinch CD, Ibhazehiebo K, Jeong JH, Habibi HR, Kurrasch DM. Low-dose exposure to bisphenol A and replacement bisphenol S induces precocious hypothalamic neurogenesis in embryonic zebrafish. Proc Natl Acad Sci U S A 2015; 112: 1475-80.

Mork L, Crump G. Zebrafish Craniofacial Development: A Window into Early Patterning. Curr Top Dev Biol 2015; 115: 235-69.